Zernike coefficients of a circular Gaussian pupil

Cosmas Mafusire and Tjaart P. J. Krüger
Department of Physics, Faculty of Natural and Agricultural Sciences, University of Pretoria,
Private Bag X20, Hatfield, 0028, South Africa.
e-mail: *cosmasmafusire@gmail.com*

Abstract

We present a derivation of a formula for Zernike-Gauss circle coefficients expressed in terms of Zernike circle coefficients for a circular Gaussian pupil by revisiting a method in which the orthonormal Zernike-Gauss circle polynomials are not derived first. This is achieved by utilizing a new result, based on the extended Nijboer-Zernike diffraction theory, in which an analytical expression for the autocorrelation of any two Zernike circle polynomials in the circular Gaussian pupils is derived. We use the result to investigate the Strehl ratio of a nearly diffraction-limited optical system that is characterized using Zernike circle coefficients or classical peak-valley coefficients. The results show that aberration correction of the system with a circular Gaussian pupil is most effective if the aberrations are expressed in terms of orthonormal Zernike-Gauss circle coefficients.

1. Introduction

It is well-established that image formation consists of information-carrying light from an imaging system passing through an exit pupil and focused onto an image plane where a point spread function (PSF) is formed [1]. This means that a PSF is nothing more than the magnitude of the Fourier transform of the pupil function, which is dependent on the pupil shape and field distribution. The classical definition of image formation consists of uniform light focused through a circular pupil, and then forming a PSF in the form of an Airy pattern. If the pupil is aberrated, the PSF shows clear deviation from the Airy shape. This deviation is determined by the aberration types and intensity distribution of the entrance pupil. Zernike circle (ZC) polynomials were invented as a way of representing phase in a unit circle. Due to their orthonormality in the unit circle, this representation includes the following advantages [2].

i. ZC polynomials can be related to classical aberrations.
ii. The mean and variance of the unit field in the pupil plane of a nearly diffraction-limited imaging system can be calculated from the ZC piston and the sum of the squared magnitude of the non-piston coefficients describing the phase of this field such that the Strehl ratio of the resultant PSF is maximised for each aberration.
iii. Each coefficient represents the contribution of the respective aberration to the wavefront's standard deviation with the advantage that the coefficient's size is not influenced by the number of terms used in the phase fitting procedure.

In contrast, a Gaussian beam transmitted through the same circular pupil generates a different PSF, even if the phase distribution is the same. The central intensity is reduced with the power going from the central lobe into the secondary rings raising their maxima slightly. The presence of aberrations has the effect of changing the shape of the PSF. This means that the Strehl ratio is not maximised and the pupil variance can no longer be expressed in terms of the ZC coefficients. This implies that the wavefront error of the pupil can no longer be calculated from the ZC coefficients [2]. To solve this problem, orthonormal Zernike-Gauss circle (ZGC) polynomials were derived in which the respective expansion coefficients could be used to recover all the advantages of orthonormality [3,4] as listed above but this time applied to a circular Gaussian pupil. Previous studies have shown that the ZGC polynomials can be derived by either performing the Gram-Schmidt orthogonalization procedure [4-12] or the Cholesky decomposition [5-12] on the ZC polynomials to transfer their properties to a new set that would take into account the circularly-diffracted Gaussian field distribution. An important parameter that was used in those derivations is the truncation factor, which is defined as the ratio of the pupil radius to the beam radius. The smaller the truncation factor, the more uniform the transmitted field. In this limit, the results agree with those of a uniform pupil in that the ZGC polynomials reduce to ZC polynomials [4].

There are two practical problems that can be solved using orthonormal polynomials. The first is that, in diffraction-limited systems, the Strehl ratio can be calculated from a simple formula based on the wavefront variance. The second is that most devices on the market capable of measuring phase are designed to use ZC polynomials. In both cases, it is necessary to convert the acquired ZC coefficients into ZGC coefficients so that the advantages of orthonormality can be restored. This is akin to changing the basis from the ZC set, in which the amplitude plays no part, to the ZGC set for the same amplitude and phase distribution. ZC polynomials belong to a special class of polynomials referred to as orthonormal Zernike-based (OZ) polynomials that are orthonormal in a general non-circular, non-uniform pupil in which the unit circle is a special, trivial case [5,6]. A generalized model that can be used to acquire such polynomials from the ZC-polynomial set using the Gram-Schmidt procedure has been in the literature for a while. These polynomials can be fitted directly onto the wavefront to generate a set of non-orthonormal coefficients. The same coefficients can also be acquired by fitting the ZC polynomials to get the respective ZC coefficients, which are then converted to orthonormal coefficients without acquiring OZ polynomials first, a method that was used in a previous study to acquire Zernike coefficients in a scaled pupil [13]. To achieve this, a matrix approach was created and is based

on deriving a positive semi-definite matrix, which is created by calculating its elements through integrating any two ZC polynomials in the general pupil [14]. Using the Cholesky method, the matrix is then decomposed into a product of a lower triangular matrix and its transpose. The rest of the calculations follow from this result. This matrix approach has proved suitable for creating numerical models which are normally implemented using computers [15,16].

In this paper, we meet two goals. The first of which is revisiting the model for the OZ formalism but this time expanding on its mathematical foundations. The second is that we derive a formula for expressing OZ coefficients in a circular Gaussian pupil which we use to analyse the implications of applying Gaussian pupils in adaptive systems. We begin by confirming that a positive semi-definite matrix is at the heart of the theory of OZ polynomials. We defer to the idea that, for all intents and purposes, each element of this matrix is an autocorrelation coefficient for each pair of ZC polynomials in that pupil. We therefore demonstrate that the matrix is, in fact, an autocorrelation matrix with usual properties such as symmetry, semi-definiteness and which possess real and positive eigenvalues. We therefore emphasise the importance of acquiring an analytical solution of the elements of such a matrix. We further demonstrate the efficacy of our method by acquiring a general solution for the auto-correlation of any two ZC polynomials in a circular Gaussian pupil. This is achieved with the help of the extended Nijboer-Zernike diffraction theory [17]. As an example, the results are then applied to the derivation of the ZGC polynomials and of the respective coefficients. The paper is organised as follows. In Section 2, we revisit the derivation of OZ polynomials where we derive a general matrix expression for the OZ polynomials from the ZC coefficients. We proceed to show how the Cholesky decomposition can be derived from the Gram-Schmidt procedure. In Section 3, we apply the model to a system with a circular Gaussian pupil in which we derive a formulation expressing ZGC coefficients in terms of ZC coefficients. We achieve this through the derivation of a new analytical expression for the inner product of any two ZC polynomials in a circular Gaussian pupil. We use this result, in Section 4, to show how different aberration coefficient definitions such as the ZC, ZGC and classical coefficients contribute to how we interpret the Strehl ratio for a circular Gaussian pupil. In the process, we demonstrate how the overfill factor affects adaptive control of optical systems with circular Gaussian pupils. In the last section, we draw conclusions. Throughout this paper, we will denote column vectors in bold lower case letters and matrices in the bold, upper case format.

2. Revisiting orthonormal Zernike-based polynomials and the associated algorithms

We are going to assume that an electric field emerges from an imaging system with a pupil of an arbitrary general shape. The field, on transmission through the pupil, can be represented by,

$$U(\boldsymbol{r}) = E(\boldsymbol{r})e^{i\phi(\boldsymbol{r})}. \tag{1}$$

This equation describes a complex pupil function that depends on the two-dimensional transverse spatial coordinates $\boldsymbol{r} = \boldsymbol{r}(\rho,\theta)$, which, in turn, are a function of cylindrical coordinates, (ρ,θ). Here, $E(\boldsymbol{r})$ and $\phi(\boldsymbol{r})$ are the real amplitude and the phase, respectively. The phase can be expressed as a linear expansion of the complete ordered orthonormal Zernike polynomial set given by the column vector, which we represent in set-builder notation, $\boldsymbol{z} = \{Z_j(\rho,\theta) \mid j,J \in \mathbb{Z}^{>}; j \le J\}$, such that

$$\phi(\boldsymbol{r}) = \boldsymbol{c}^{\boldsymbol{t}}\boldsymbol{z}, \tag{2}$$

where we choose to represent the wavefront using the first J ZC polynomials and $^{\boldsymbol{t}}$ represents matrix or vector transposition. Here, each coefficient is part of a set, $\boldsymbol{c} = \{C_j \in \mathbb{R} \mid j,J \in \mathbb{Z}^{>}; j \le J\}$ such that it has an associated ZC polynomial, $\mathrm{Z}_j(\rho,\theta)$. Using cylindrical coordinates, each ZC polynomial is given by a product of a radial and an azimuthal term such that

$$\begin{aligned} Z_j(\rho,\theta) &= Z_n^m(\rho,\theta) = \sqrt{n+1}R_n^{|m|}(\rho)\Theta^m(\theta) \\ &= \sqrt{n+1}\sum_{s=0}^{p}(-1)^s \binom{n-s}{s\quad q-s\quad p-s} \rho^{n-2s} \begin{cases} \sqrt{2-\delta_{|m|,0}}\cos m\theta, & m \ge 0, \\ \sqrt{2}\sin|m|\theta, & m < 0 \end{cases} \end{aligned} \tag{3}$$

where $p = \frac{1}{2}(n-|m|)$ and $q = \frac{1}{2}(n+|m|)$. Note that the radial polynomial is expressed in terms of trinomial coefficients. The ZC set is a sequence, usually ordered with an arrangement indicated by j, sometimes referred to as the Noll sequence, [18] where each value of which has an associated unique double index set (n,m) with n and m being the order and azimuthal numbers, respectively, where [19]

$$n = \left\lceil \frac{\sqrt{8j+1}-3}{2} \right\rceil; \quad m = (-1)^{\mathrm{mod}(j,2)}\left(n - 2\left\lfloor \frac{(n+1)(n+2)-2j}{4} \right\rfloor \right) \tag{4}$$

Note that the second equation has been slightly modified from the one in the original reference to account for the second piecewise condition, $m < 0$, in Eq. (3). The single index can be reacquired from the double index using the equation [20]

$$j = \begin{cases} \delta_{\mathrm{mod}\{(n-|m|),2\},0}\left(\dfrac{n(n+1)}{2} + |m| + \begin{cases} 1, & m \le 0 \wedge 0 \le \mathrm{mod}(n,4) \le 1 \\ 1, & m \ge 0 \wedge 2 \le \mathrm{mod}(n,4) \le 3 \\ 0, & m < 0 \wedge 2 \le \mathrm{mod}(n,4) \le 3 \\ 0, & m > 0 \wedge 0 \le \mathrm{mod}(n,4) \le 1 \end{cases} \right), & n \ge |m| \\ 0, & n < |m| \end{cases} . \tag{5}$$

which has also been modified. As such, an alternative representation of the ZC set is then expressed in form of the set builder notation, $\boldsymbol{z} = \{Z_n^m(\rho,\theta) \mid (n,m) \in \mathbb{Z}^{\geq} \times \mathbb{Z}; \frac{1}{2}(n-|m|) \in \mathbb{Z}^{\geq}; (n,m) \le (N,M)\}$. It is assumed that J has associated order numbers, (N,M). ZC polynomials are orthonormal in a unit circular disc such that the expansion coefficients can be used to give the wavefront mean and variance from the piston and the sum of the square of the non-piston terms, respectively.

However, since the general pupil is amplitude-weighted and of arbitrary shape, the ZC set would not be orthonormal, a drawback which can be overcome by deriving a respective OZ polynomial set that meets the orthonormality criterion. An OZ set, represented as $\boldsymbol{o} = \{O_j(\boldsymbol{r}) \mid j, J \in \mathbb{Z}^{>}; j \le J\}$ is such that the phase function in Eq. (2) can be alternatively presented as

$$\phi(\boldsymbol{r}) = \boldsymbol{x}^t \boldsymbol{o}\,, \tag{6}$$

making $\boldsymbol{x} = \{X_j \in \mathbb{R} \mid j, J \in \mathbb{Z}^{>}; j \le J\}$ an ordered set of the respective expansion coefficients. As expected, the OZ set is orthonormal in the general pupil and so the inner product of any two polynomials of the set in the pupil has the property,

$$\frac{\iint_A \boldsymbol{o}\boldsymbol{o}^t E(\boldsymbol{r}) d^2\boldsymbol{r}}{\iint_A E(\boldsymbol{r}) d^2\boldsymbol{r}} = \boldsymbol{I}\,, \tag{7}$$

where A depicts the boundary of the general pupil. Eq. (7) implies that the OZ set is orthonormal due to the result being an identity matrix and its non-singularity tells us that the set is linearly independent. This indicates that this set forms the basis of the vector space described by the general pupil. Therefore, each coefficient will be an element of the vector,

$$\boldsymbol{x} = \frac{\iint_A \boldsymbol{o}\phi(\boldsymbol{r}) E(\boldsymbol{r}) d^2\boldsymbol{r}}{\iint_A E(\boldsymbol{r}) d^2\boldsymbol{r}}\,. \tag{8}$$

It has been established that any OZ set can be derived from ZC polynomials using the Gram-Schmidt procedure as shown by the recursive calculation [10]

$$O_j(\boldsymbol{r}) = \frac{1}{g_{jj}}\left(Z_j(\rho,\theta) - \sum_{j'=1}^{j-1} g_{jj'} O_{j'}(\boldsymbol{r}) \right). \tag{9}$$

Note that the calculation of the normalizing coefficient, $1/g_{jj}$, is based on the orthonormality of the set $\boldsymbol{o}$ as defined by Eq. (7), a property that has been extensively discussed in the literature [3,4,7]. In addition, $g_{jj'} \in \boldsymbol{G}$ such that $\boldsymbol{G} = \{g_{jj'} \in \mathbb{R} \mid j, j', J \in \mathbb{Z}^{>}; j' \le j \le J\}$, a lower triangular matrix operationally defined by

$$\boldsymbol{G} = \frac{\iint_A \boldsymbol{z}\boldsymbol{o}^t E(\boldsymbol{r}) d^2\boldsymbol{r}}{\iint_A E(\boldsymbol{r}) d^2\boldsymbol{r}}\,. \tag{10}$$

As a result, the wavefront mean and variance of a weakly aberrated general pupil can be found by the respective expressions

$$\langle \phi(\boldsymbol{r}) \rangle = \boldsymbol{x}^t \boldsymbol{e}_1 \,;\; \sigma_\phi^2 = \langle [\phi(\boldsymbol{r})]^2 \rangle - \langle \phi(\boldsymbol{r}) \rangle^2 = \boldsymbol{x}^t (\boldsymbol{I} - \boldsymbol{e}_1 \boldsymbol{e}_1^t) \boldsymbol{x} \,, \tag{11}$$

which are solved by calculating the integral

$$\langle [\phi(\boldsymbol{r})]^\alpha \rangle = \frac{\iint_A [\phi(\boldsymbol{r})]^\alpha E(\boldsymbol{r}) d^2\boldsymbol{r}}{\iint_A E(\boldsymbol{r}) d^2\boldsymbol{r}} \,, \tag{12}$$

and by inserting $\alpha = 1$ and 2, respectively into Eq. (12). The vector $\boldsymbol{e}_1^t = \{1, 0, 0, 0 \ldots 0\}$ is the first vector in a standard basis of a J -dimensional Euclidean space. As such, the amplitude-weighted Strehl ratio [21]

$$S_E = \left| \frac{\iint_A e^{i\phi(\boldsymbol{r})} E(\boldsymbol{r}) d^2\boldsymbol{r}}{\iint_A E(\boldsymbol{r}) d^2\boldsymbol{r}} \right|^2 \cong \exp(-\sigma_\phi^2) \,, \tag{13}$$

which, as we show, can be approximated by the Gaussian empirical formula if we assume a nearly diffraction-limited optical system.

Once $\boldsymbol{o}$ has been acquired, a direct relationship between the two coefficient systems can be derived. The motivation is that it is always easier to fit ZC polynomials to the phase until we get a sufficient number of coefficients to accurately reconstruct the phase as depicted by Eq. (2). If the relationship between $\boldsymbol{c}$ and $\boldsymbol{x}$ can be derived, then after fitting the ZC set, the OZ set can be calculated such that mean and variance can be acquired. It can be easily verified that this relationship is given by

$$\boldsymbol{x} = \boldsymbol{G}^t \boldsymbol{c} \,. \tag{14}$$

Note that each OZ coefficient is a sum of a linear combination of ZC coefficients starting with one of the same order and higher up to J given that $\boldsymbol{G}^t$ is an upper triangular matrix.

Alternatively, we can calculate $\boldsymbol{G}$ without determining $\boldsymbol{o}$ by expressing $\boldsymbol{z}$ (i.e. the ZC set) as a linear combination of the OZ polynomials:

$$\boldsymbol{z} = \boldsymbol{G}\boldsymbol{o} \,. \tag{15}$$

We then eliminate $\boldsymbol{o}$ from Eqs. (7) and (15) leading to

$$\boldsymbol{B} = \boldsymbol{G}\boldsymbol{G}^t = \frac{\iint_A \boldsymbol{z}\boldsymbol{z}^t E(\boldsymbol{r}) d^2\boldsymbol{r}}{\iint_A E(\boldsymbol{r}) d^2\boldsymbol{r}} \,, \tag{16}$$

a square matrix which we can calculate by integrating a product of ZC polynomials in the general pupil in which $\boldsymbol{B} = \{\beta_{jj'} \in \mathbb{R} \mid j, j', J \in \mathbb{Z}^>; j', j \le J\}$. Also note that a direct comparison of Eqs. (10) and (14) leads to

$$\boldsymbol{G}\boldsymbol{e}_1 = \boldsymbol{B}\boldsymbol{e}_1 \,, \tag{17}$$

i.e., the first columns of $\boldsymbol{G}$ and $\boldsymbol{B}$ are identical. $\boldsymbol{B}$ can be defined as a matrix whose elements consist of the correlation coefficients of the ZC polynomials, $Z_j(\rho, \theta)$ and $Z_{j'}(\rho, \theta)$, in the general pupil. When $\beta_{jj'} = 0$, it implies that the respective aberrations, $Z_j(\rho, \theta)$ and $Z_{j'}(\rho, \theta)$, are uncorrelated in this pupil. Furthermore, $\boldsymbol{B}$ possesses the properties that are exhibited by an autocorrelation matrix i. e.,

i. It is symmetrical because it is evident that $\boldsymbol{B}^t = \boldsymbol{B}$.
ii. It is positive semidefinite in that for some vector $\boldsymbol{c}$, which, in this case, happens to be the vector containing the ZC coefficients, $\boldsymbol{c}^t \boldsymbol{B} \boldsymbol{c} = \boldsymbol{c}^t \boldsymbol{G}\boldsymbol{G}^t \boldsymbol{c} = \boldsymbol{x}^t \boldsymbol{x} \ge 0$.
iii. The eigenvalue of $\boldsymbol{B}$, λ, is always real and non-negative in that for the same vector, $\boldsymbol{c}$, the matrix eigenvalue, λ, fulfils the equation $\boldsymbol{B}\boldsymbol{c} = \lambda \boldsymbol{c}$. To prove this, we express the equation in the form $\boldsymbol{c}^t \boldsymbol{B} \boldsymbol{c} = \lambda \boldsymbol{c}^t \boldsymbol{c}$ from which we get an expression for the eigenvalue, $\lambda = \dfrac{\boldsymbol{x}^t \boldsymbol{x}}{\boldsymbol{c}^t \boldsymbol{c}} \ge 0$, on the condition that $\boldsymbol{c}^t \boldsymbol{c} > 0$.

The above-given properties imply that $\boldsymbol{B}$ fulfils the necessary conditions to undergo successful Cholesky decomposition, the result of which we designate

$$\boldsymbol{G} = \mathcal{C}\mathcal{D}[\boldsymbol{B}] \,. \tag{18}$$

The algorithm required to perform this task is widely available in the literature [22] but we provide a derivation that can be linked directly to the Gram-Schmidt procedure. We do this by calculating through premultiplying Eq. (7) by $Z_i(\rho,\theta)$, integrating in the general pupil and interchanging the subscripts i, j and j' accordingly, after simplifying using $g_{jj'} \in \boldsymbol{G}$ in Eq. (8). The result is a recursive expression that defines a particular version of the Cholesky decomposition algorithm, namely, the Cholesky–Banachiewicz variation given by [23,24]

$$g_{jj'} = \begin{cases} \dfrac{1}{g_{j'j'}}\left(\beta_{jj'} - \displaystyle\sum_{i=1}^{j'-1} g_{j'i} g_{ji}\right), & j' < j \\ 0, & j' > j \\ \sqrt{\beta_{jj} - \displaystyle\sum_{i=1}^{j-1} (g_{ji})^2}, & j' = j \end{cases}, \tag{19}$$

in which $\boldsymbol{G}$ is filled in row by row and from left to right up to the diagonal, with zeroes filling the rest as opposed to going column by column. We see that the g parameters are derived from the β parameters as defined by Eq. (16) using the Cholesky decomposition as defined by Eq. (19). Note that this is also a recursive algorithm in which each g parameter, through successive substitutions, can be expressed in terms of lower-order realisations of β parameters.

This implies that if one can get an analytical solution of Eq. (16), each coefficient can be determined by making the substitutions of the appropriate indices, n and m. This method is more efficient than to calculate each coefficient individually. Furthermore, if one can express any problem in terms of $\boldsymbol{B}$, then it becomes possible to solve it once $\boldsymbol{B}$ has been found. It is apparent that we can present the mean and the variance of the phase as given by Eq. (11), in terms of the ZC coefficients using Eq. (14). However, if we then simplify the resulting expression further using Eqs. (16) and (17), the result is shown to be

$$\langle \phi(\boldsymbol{r}) \rangle = \boldsymbol{c}^t \boldsymbol{B} \boldsymbol{e}_1 \; ; \; \sigma_\phi^2 = \boldsymbol{c}^t (\boldsymbol{B} - \boldsymbol{B}\boldsymbol{e}_1 \boldsymbol{e}_1^t \boldsymbol{B}) \boldsymbol{c} \, . \tag{20}$$

Therefore the mean and variance of the field, in discrete form, can be represented by

$$\langle \phi(\boldsymbol{r}) \rangle = \sum_{j=1}^{J} C_j \beta_{1j} \; ; \; \sigma_\phi^2 = \sum_{j=2}^{J} \sum_{j'=j}^{J} \left((C_{j'})^2 [\beta_{j'j'} - (\beta_{1j'})^2] + 2(1-\delta_{jj'}) C_j C_{j'} (\beta_{jj'} - \beta_{1j}\beta_{1j'}) \right) . \tag{21}$$

This means that the mean of the phase is given by the sum of the ZC coefficients, each one weighted by the respective correlation coefficient for which $\beta_{1j} \neq 0$. Here we see that the variance can be split into two terms corresponding to $j' = j$ and $j' > j$. As such, each coefficient product is weighted by $\beta_{jj'} - \beta_{1j}\beta_{1j'}$, the amplitude-weighted covariance of the respective ZC polynomials, Z_j and $Z_{j'}$, with $\beta_{jj} - (\beta_{1j})^2$ being the amplitude-weighted variance of an individual polynomial, Z_j, which can be used as a measure of the coupling effect between two aberrations. They reduce to a value of 1 and 0, respectively, in the limit of the unit circle, and thus the variance as defined in Eq. (11), is realised. The OZ polynomials themselves can then be constructed by

$$\boldsymbol{o} = (\boldsymbol{C}\mathcal{D}[\boldsymbol{B}])^t \boldsymbol{z} \, . \tag{22}$$

Note that $g_{11} = \beta_{11} = 1$. In the limit of a unit circle, $\boldsymbol{G} = \boldsymbol{B} = \boldsymbol{I}$, which we can use in Eqs. (14) and (15) to verify that for the coefficients and the polynomials, $\boldsymbol{x} \to \boldsymbol{c}$ and $\boldsymbol{o} \to \boldsymbol{z}$, respectively. We can also demonstrate that Eqs. (2) and (6) are equivalent to each other by taking $\boldsymbol{x}^t \boldsymbol{o}$ as defined by Eq. (6) and replacing $\boldsymbol{x}$ and $\boldsymbol{o}$ with $\boldsymbol{G}^t \boldsymbol{c}$ and $\boldsymbol{G}^{-1} \boldsymbol{z}$, respectively, as illustrated by Eqs. (14) and (15). The result is Eq. (2), which proves our assertion. The result is based on the idea that $\boldsymbol{G}$ is a square lower-triangular non-singular matrix of dimension $J \times J$ where $j = J$ is the highest order of the ZC term used in the fitting procedure. This implies that the resultant expansion expressed in terms of the OZ polynomials would also have the highest order $j = J$ in order for the original wavefront to be completely represented so that it can be accurately reconstructed.

3. Aberrations of the circular Gaussian pupil

We now apply the above theory to optical systems with circular Gaussian pupils. We are going to assume that the light field of interest has a radius ω on entering an exit circular pupil that is set to allow the transmission of limited amplitude and phase. Provisionally, let us assume a Gaussian field transmitted through an exit pupil with an electric field function is given by

$$U(\rho,\theta;\eta)=\begin{cases} e^{-\rho^2/\eta^2+i\phi(\rho,\theta;\eta)}; & \rho\le 1 \\ 0; & \rho>0 \end{cases}. \tag{23}$$

In Eq. (23), U is a complex pupil function that depends on the two-dimensional transverse spatial cylindrical coordinates (ρ,θ) and the overfill factor $\eta=\omega/a$. Note that η is a reciprocal of the square root of the truncation factor [3-6,10]. It can be used to define diffraction regimes depending on the amount of edge diffraction.

i. We identify the untruncated pupil as the one in which the Gaussian beam is transmitted through circular pupil with minimal to no edge diffraction. According to Mahajan, for an aberrated Gaussian beam, an underfilled pupil is when $\eta\le 1/3$ [4] when the beam would be transmitted while retaining its Gaussian shape and so it would experience minimal to no edge diffraction.

ii. We define the underfilled pupil as one in which $1/3\le\eta\le 2$ and is somewhere between the untruncated and overfilled pupils.

iii. An overfilled pupil can be described as satisfying the condition $2\le\eta<\infty$ where we define η as having a large but finite value. This results in excessive edge diffraction whilst transmitting very little energy.

iv. As $\eta\to\infty$, the result is a uniform field which is sometimes referred to as the truncated plane wave, the theoretical limit depicting an extremely overfilled Gaussian pupil. If we insert this limit in our formulation, the ZC formulation is recovered.

In Eq. (23), the phase distribution of the Gaussian pupil, $\phi(\rho,\theta;\eta)$, can be expressed as a linear expansion of the complete and ordered ZGC polynomials, $\{\mathrm{Z}_n^m(\rho,\theta;\eta)\}$, or in terms of the ZC set, $\{\mathrm{Z}_n^m(\rho,\theta)\}$. Let us suppose that the phase is fitted with a function composed of a finite set of ZC coefficients comprising the set $\{C_n^m\}$ up to some preselected order J, which has the associated order numbers (N,M) such that its reconstruction is given by $\sum_{j(n,m)=1}^{J(N,M)} C_n^m\,\mathrm{Z}_n^m(\rho,\theta)$. The same phase can also be represented in terms of ZGC polynomials such that the phase is given by $\sum_{j(n,m)=1}^{J(N,M)} X_n^m\,\mathrm{Z}_n^m(\rho,\theta;\eta)$, where $\{X_n^m\}$ is the respective coefficient set.

a. The β parameter and the Zernike-Gauss circle polynomials

The β parameter for the circular Gaussian pupil is calculated from an inner product of a pair of ZC polynomials in a circular Gaussian pupil and is given by

$$\begin{aligned}\beta_{n,n'}^{|m|}&=\frac{\int_0^{2\pi}\int_0^1 Z_n^m(\rho,\theta)Z_{n'}^{m'}(\rho,\theta)e^{-\rho^2/\eta^2}\rho d\rho d\theta}{\int_0^{2\pi}\int_0^1 e^{-\rho^2/\eta^2}\rho d\rho d\theta}\\ &=\delta_{m,m'}\frac{(-1)^{p+p'}\sqrt{(n+1)(n'+1)}}{e^{1/\eta^2}-1}\sum_{l=1}^{\infty}\sum_{s=0}^{p'}\frac{2s+l+|m|}{l!l\eta^{2l}}\frac{\binom{s+l+|m|-1}{l-1}\binom{s+l-1}{l-1}\binom{l-1}{p-s}\binom{l-1}{p'-s}}{\binom{s+l+q}{l}\binom{s+l+q'}{l}}\\ &=\delta_{m,m'}\frac{(-1)^{p}\sqrt{(n+1)(n'+1)}}{1-e^{-1/\eta^2}}\sum_{s=0}^{p'}(-1)^s\binom{n'-s}{s\quad p'-s\quad q'-s}\eta^{2(q'-s)}G_{2,3}^{2,1}\left(\frac{1}{\eta^2}\middle|\begin{matrix}1 & |m|+1\\ q+1 & q'-s+1 & -p\end{matrix}\right)\end{aligned}, \tag{24}$$

a solution presented in two equivalent forms. It is nonzero when $n'=|m|,|m|+2,\ldots,n$ and G represents the Meijer G–function with $p'=\frac{1}{2}(n'-|m|)$ and $q'=\frac{1}{2}(n'+|m|)$. The separate derivations of the two equivalent forms are outlined in Appendix A with the first one partly achieved by using a result from the extended Zernike-Nijboer theory [21] though it is possible to derive the second directly from the first, that approach was avoided here. Eq. (24) allows us to generate ZGC polynomials and the respective coefficients from the respective ZC counterparts, analytically, through the repeated use of Eq. (24) by inserting the respective indices. The β parameters required for the derivation of the first 11 ZGC polynomials coefficients and their corresponding coefficients are

$$\beta_{0,0}^{0}=1;\qquad \beta_{1,1}^{1}=2\left(\eta^2+\frac{1}{1-\mathrm{e}^{1/\eta^2}}\right)\cong 2\eta^2;\qquad \beta_{2,0}^{0}=\sqrt{3}\left(2\eta^2-\coth\left(\frac{1}{2\eta^2}\right)\right)\cong\sqrt{3}(2\eta^2-1);$$

$$\beta_{2,2}^{0}=3\left(8\eta^4-4\eta^2\coth\left(\frac{1}{2\eta^2}\right)+1\right)\cong 3(8\eta^4-4\eta^2+1);\qquad \beta_{2,2}^{2}=3\left(2\eta^4+\frac{2\eta^2+1}{1-\mathrm{e}^{1/\eta^2}}\right)\cong 6\eta^4;$$

$$\beta_{3,1}^{1}=2\sqrt{2}\left(6\eta^4-2\eta^2+\frac{6\eta^2+1}{1-\mathrm{e}^{1/\eta^2}}\right)\cong 4\sqrt{2}\eta^2(3\eta^2-1);\qquad \beta_{3,3}^{3}=4\left(6\eta^6+\frac{6\eta^4+3\eta^2+1}{1-\mathrm{e}^{1/\eta^2}}\right)\cong 24\eta^6;$$

$$\beta_{3,3}^{1}=4\left(54\eta^6-24\eta^4+4\eta^2+\frac{54\eta^4+3\eta^2+1}{1-\mathrm{e}^{1/\eta^2}}\right)\cong 8\eta^2(27\eta^4-12\eta^2+2);$$

$$\beta_{4,0}^{0}=\sqrt{5}\left(12\eta^4-6\eta^2\coth\left(\frac{1}{2\eta^2}\right)+1\right)\cong\sqrt{5}(12\eta^4-6\eta^2+1);$$

$$\beta_{4,2}^{0}=\sqrt{15}\left(8\eta^2(9\eta^4+1)-(36\eta^4+1)\coth\left(\frac{1}{2\eta^2}\right)\right)\cong\sqrt{15}[8\eta^2(9\eta^4+1)-(36\eta^4+1)];$$

$$\beta_{4,4}^{0}=5\left(96\eta^4(9\eta^4+1)-12\eta^2(36\eta^4+1)\coth\left(\frac{1}{2\eta^2}\right)+1\right)\cong 5[96\eta^4(9\eta^4+1)-12\eta^2(36\eta^4+1)+1].\qquad \textbf{(25)}$$

Each of these has been further simplified resulting in an approximate result representing an untruncated pupil.

The ZGC polynomials can then be derived by expressing them in terms of the ZC polynomials where expansion coefficients are constructed using the β parameters as depicted by Eq. (22). The results for all the aberrations up to $(n,m)=(4,0)$ which is when $j=11$, are given by

$$Z_0^0(\rho,\theta;\eta)=1;\quad Z_1^{\pm1}(\rho,\theta;\eta)=\frac{Z_1^{\pm1}(\rho,\theta)}{\sqrt{\beta_{1,1}^{1}}};\quad Z_2^0(\rho,\theta;\eta)=\frac{Z_2^0(\rho,\theta)-\beta_{2,0}^{0}}{\sqrt{\beta_{2,2}^{0}-(\beta_{2,0}^{0})^2}};\quad Z_2^{\pm2}(\rho,\theta;\eta)=\frac{Z_2^{\pm2}(\rho,\theta)}{\sqrt{\beta_{2,2}^{2}}};$$

$$Z_3^{\pm1}(\rho,\theta;\eta)=\frac{Z_3^{\pm1}(\rho,\theta)-\dfrac{\beta_{3,1}^{1}}{\beta_{1,1}^{1}}Z_1^{\pm1}(\rho,\theta)}{\sqrt{\beta_{3,3}^{1}-\dfrac{(\beta_{3,1}^{1})^2}{\beta_{1,1}^{1}}}};\quad Z_3^{\pm3}(\rho,\theta;\eta)=\frac{Z_3^{\pm3}(\rho,\theta)}{\sqrt{\beta_{3,3}^{3}}};$$

$$Z_4^0(\rho,\theta;\eta)=\frac{Z_4^0(\rho,\theta)-\dfrac{\beta_{4,2}^{0}-\beta_{4,0}^{0}\beta_{2,0}^{0}}{\beta_{2,2}^{0}-(\beta_{2,0}^{0})^2}(Z_2^0(\rho,\theta)-\beta_{2,0}^{0})-\beta_{4,0}^{0}}{\sqrt{\beta_{4,4}^{0}-(\beta_{4,0}^{0})^2-\dfrac{(\beta_{4,2}^{0}-\beta_{4,0}^{0}\beta_{2,0}^{0})^2}{\beta_{2,2}^{0}-(\beta_{2,0}^{0})^2}}},\qquad \textbf{(26)}$$

where the $\pm$ sign refer to the *x*- and *y*-aberrations corresponding to the + and – signs, respectively. Note that the above equations can be manipulated further if we express ZC polynomials in terms of cylindrical or Cartesian coordinates as needed, to get corresponding expressions for the ZGC polynomials. The corresponding radial polynomials for an overfilled pupil can be acquired by inserting the approximate results in Eq. (25) and simplifying the result through eliminating the angular part and the normalising coefficients to get

$$R_0^0(\rho;\eta)=1;\quad R_1^1(\rho;\eta)=\frac{\rho}{\sqrt{2}\eta};\quad R_2^0(\rho;\eta)=\frac{1}{\sqrt{3}}\left(\frac{\rho^2}{\eta^2}-1\right);\quad R_2^2(\rho;\eta)=\frac{\rho^2}{\sqrt{6}\eta^2};\quad R_3^1(\rho;\eta)=\frac{1}{2\sqrt{2}}\left(\frac{\rho^3}{\eta^3}-2\frac{\rho}{\eta}\right);$$

$$R_3^3(\rho;\eta)=\frac{\rho^3}{6\eta^3};\quad R_4^0(\rho;\eta)=\frac{1}{2\sqrt{5}}\left(\frac{\rho^4}{\eta^4}-4\frac{\rho^2}{\eta^2}+2\right).\qquad \textbf{(27)}$$

The results of Eqs (24) and (27) match those acquired by Mahajan in which he used a recursive Gram-Schmidt calculation (see Eq. (9)), expressing the results in terms of selected truncation factors, [4] thereby validating our approach. The triangular astigmatism approximation is presented here, perhaps for the first time.

b. Zernike circle, Zernike-Gauss circle and classical coefficients in a circular Gaussian pupil

To convert the ZC coefficients into the ZGC set, we use Eq. (14). The resulting coefficients, X_n^m, are to be calculated using the expression

$$X_n^m = \sqrt{\beta_{n,n}^{|m|} - \sum_{i=|m|}^{n-2} (g_{n,i}^{|m|})^2}\, C_n^m + \sum_{n'=n+2}^{N} \frac{1}{g_{n',n'}^{|m|}} \left(\beta_{n,n'}^{|m|} - \sum_{i=|m|}^{n'-2} g_{n',i}^{|m|} g_{n,i}^{|m|} \right) C_{n'}^m \qquad \textbf{(28)}$$

by searching all the coefficients of order numbers $n' = n, n+2, \ldots, N$. The ZGC coefficients expressed in terms of ZC coefficients up to $j = 11$ are shown to be

$$X_0^0 = C_0^0 + \beta_{2,0}^0 C_2^0 + \beta_{4,0}^0 C_4^0 \cong C_0^0 + \sqrt{3}(2\eta^2 - 1)C_2^0 + \sqrt{5}(12\eta^4 - 6\eta^2 + 1)C_4^0;$$

$$X_1^{\pm 1} = \sqrt{\beta_{1,1}^1}\, C_1^{\pm 1} + \frac{\beta_{3,1}^1}{\sqrt{\beta_{1,1}^1}} C_3^{\pm 1} \cong \sqrt{2}\eta C_1^{\pm 1} + 4\eta(3\eta^2 - 1)C_3^{\pm 1};$$

$$X_2^0 = \sqrt{\beta_{2,2}^0 - (\beta_{2,0}^0)^2}\, C_2^0 + \frac{\beta_{4,2}^0 - \beta_{4,0}^0 \beta_{2,0}^0}{\sqrt{\beta_{2,2}^0 - (\beta_{2,0}^0)^2}} C_4^0 \cong 2\sqrt{3}\eta^2 C_2^0 + 6\sqrt{5}\eta^2(4\eta^2 - 1)C_4^0;\ X_2^{\pm 2} = \sqrt{\beta_{2,2}^2}\, C_2^{\pm 2} \cong \sqrt{6}\eta^2 C_2^{\pm 2};$$

$$X_3^{\pm 1} = \sqrt{\beta_{3,3}^1 - \frac{(\beta_{3,1}^1)^2}{\beta_{1,1}^1}}\, C_3^{\pm 1} \cong 6\sqrt{2}\eta^3 C_3^{\pm 1};\ X_3^{\pm 3} = \sqrt{\beta_{3,3}^3}\, C_3^{\pm 3} \cong 2\sqrt{6}\eta^3 C_3^{\pm 3};$$

$$X_4^0 = \sqrt{\beta_{4,4}^0 - (\beta_{4,0}^0)^2 - \frac{(\beta_{4,2}^0 - \beta_{4,0}^0 \beta_{2,0}^0)^2}{\beta_{2,2}^0 - (\beta_{2,0}^0)^2}}\, C_4^0 \cong 12\sqrt{5}\eta^4 C_4^0. \qquad \textbf{(29)}$$

The phase can also be represented in terms of primary classical aberrations, namely spherical aberration, coma, astigmatism, defocus, and tilt, in which each function is represented by the respective classical peak-valley coefficients, A_4^0, A_3^1, A_2^2, A_2^0 and A_1^1, where the phase expansion can thus be presented as

$$\phi(\rho, \theta; \eta) = A_1^1 \rho \cos\theta + A_2^0 \rho^2 + A_2^2 \rho^2 \cos^2\theta + A_3^1 \rho^3 \cos\theta + A_4^0 \rho^4. \qquad \textbf{(30)}$$

The ZC coefficients can be expressed in terms of primary classical coefficients [10]

$$C_0^0 = \frac{A_2^0}{2} + \frac{A_2^2}{4} + \frac{A_4^0}{3};\ C_1^1 = \frac{A_1^1}{2} + \frac{A_3^1}{3};\ C_2^0 = \frac{A_2^0}{2\sqrt{3}} + \frac{A_2^2}{4\sqrt{3}} + \frac{A_4^0}{2\sqrt{3}};\ C_2^2 = \frac{A_2^2}{2\sqrt{6}};\ C_3^1 = \frac{A_3^1}{6\sqrt{2}};\ C_4^0 = \frac{A_4^0}{6\sqrt{5}} \qquad \textbf{(31)}$$

with the other ZC coefficients, $C_1^{-1} = C_2^{-2} = C_3^{-1} = C_3^{-3} = C_3^3 = 0$ making this conversion incomplete with the implication here being that the wavefront constructed using Eq. (30) is now subject to error [12]. The acquired ZC coefficients can then be inserted into Eqs. (29) to express the ZGC coefficients in terms of the classical coefficients.

c. Strehl ratio of a diffraction-limited circular Gaussian pupil

We have established that, in terms of the ZGC coefficients, the wavefront mean and variance are given by the ZGC piston and the sum of the square of the non-piston ZGC coefficients. By using the coefficients in Eq. (29), we can show the mean and variance can be expressed in terms of the ZC coefficients as in

$$\langle \phi \rangle = \sum_{n=0}^{N} C_n^0 \beta_{n,0}^0;\ \sigma_\phi^2 = \begin{cases} \sum_{n=1}^{N} \sum_{m=-n}^{n} \sum_{n'=n}^{N} [(C_{n'}^m)^2 \beta_{n',n'}^{|m|} + 2(1-\delta_{n,n'}) C_n^m C_{n'}^m \beta_{n,n'}^{|m|}], & m \neq 0 \\ \sum_{n=1}^{N} \sum_{n'=n}^{N} \left\{ (C_{n'}^0)^2 [\beta_{n',n'}^0 - (\beta_{n',0}^0)^2] + 2(1-\delta_{n,n'}) C_n^0 C_{n'}^0 (\beta_{n,n'}^0 - \beta_{n,0}^0 \beta_{n',0}^0) \right\}, & m = 0 \end{cases} \qquad \textbf{(32)}$$

where $\beta_{n,n}^0 - (\beta_{n,0}^0)^2$ and $\beta_{n,n'}^0 - \beta_{n,0}^0 \beta_{n',0}^0$ are the variances and the covariances, respectively, of the rotationally symmetric ZC polynomials (i.e. when $m = 0$) in the general pupils since they are the only aberrations that correlate with piston. Therefore, for nonsymmetric aberration polynomials, which is when $m \neq 0$, $\beta_{n,n'}^{|m|}$ and $\beta_{n,n}^{|m|}$ have the same function as when $m = 0$. From the variance we can calculate the amplitude-weighted Strehl ratio, $S(\eta)$, by inserting the variance expressed in terms of Eq. (32) into Eq. (13). Here we see that the square of each orthonormal

coefficient, $(X_n^{|m|})^2$ depends on all ZC aberrations of the same azimuthal order m but of order n and higher, up to the order stipulated by the selected J.

Table 1. Breakdown of the square of the first 11 Zernike-Gauss circle coefficients expressed in terms of Zernike circle coefficients.

$(X_n^m)^2$	Squared primary term	Balancing term	Conjugate of the balancing term	Cross term
$(X_0^0)^2$	$(C_0^0)^2$		$(\beta_{2,0}^0 C_2^0)^2 + (\beta_{4,0}^0 C_4^0)^2$	$2(\beta_{2,0}^0 C_0^0 C_2^0 + \beta_{4,0}^0 C_0^0 C_4^0 + \beta_{2,0}^0 \beta_{4,0}^0 C_2^0 C_4^0)$
$(X_1^{\pm1})^2$	$\beta_{1,1}^1 (C_1^{\pm1})^2$		$\frac{(\beta_{3,1}^1)^2}{\beta_{1,1}^1}(C_3^{\pm1})^2$	$2\beta_{3,1}^1 (C_1^{\pm1} C_3^{\pm1})$
$(X_2^0)^2$	$\beta_{2,2}^0 (C_2^0)^2$	$-(\beta_{2,0}^0 C_2^0)^2$	$\frac{(\beta_{4,2}^0 - \beta_{4,0}^0 \beta_{2,0}^0)^2}{\beta_{2,2}^0 - (\beta_{2,0}^0)^2}(C_4^0)^2$	$2(\beta_{4,2}^0 - \beta_{4,0}^0 \beta_{2,0}^0) C_2^0 C_4^0$
$(X_2^{\pm2})^2$	$\beta_{2,2}^2 (C_2^{\pm2})$			
$(X_3^{\pm1})^2$	$\beta_{3,3}^1 (C_3^{\pm1})^2$	$-\frac{(\beta_{3,1}^1)^2}{\beta_{1,1}^1}(C_3^{\pm1})^2$		
$(X_3^{\pm3})^2$	$\beta_{3,3}^3 (C_3^{\pm3})^2$			
$(X_4^0)^2$	$\beta_{4,4}^0 (C_4^0)^2$	$-\frac{(\beta_{4,2}^0 - \beta_{4,0}^0 \beta_{2,0}^0)^2}{\beta_{2,2}^0 - (\beta_{2,0}^0)^2}(C_4^0)^2 - (\beta_{4,0}^0 C_4^0)^2$		

The variance contributed by each ZGC coefficient up to spherical aberration can determined by setting the limit of in Eq. (30) at $J = 11$, leading to the result:

$$\sigma_\phi^2 = \beta_{1,1}^1[(C_1^1)^2 + (C_1^{-1})^2] + [\beta_{2,2}^0 - (\beta_{2,0}^0)^2](C_2^0)^2 + \beta_{2,2}^2[(C_2^2)^2 + (C_2^{-2})^2] + \beta_{3,3}^1[(C_3^1)^2 + (C_3^{-1})^2] + \beta_{3,3}^3[(C_3^3)^2 + (C_3^{-3})^2] + [\beta_{4,4}^0 - (\beta_{4,0}^0)^2](C_4^0)^2 + 2\beta_{3,1}^1(C_1^1 C_3^1 + C_1^{-1} C_3^{-1}) + 2(\beta_{4,2}^0 - \beta_{4,0}^0 \beta_{2,0}^0) C_2^0 C_4^0 \quad \textbf{. (33)}$$

From the above equation, we ascertain that with some of the aberrations, lower-order ZC terms have been added to maximise the Strehl ratio of the PSF associated with that aberration in a process is called balancing. We illustrate this process by using an alternative calculation of the variance in which we take the square of each coefficient in Eq. (26) to acquire Eq. (29) as shown in the first column of Table 1 in appendix B. The result is that each coefficient has a squared primary term of the form $\beta_{n,n}^m (C_n^m)^2$, as shown in the second column of Table 1. However, we see that there are four ZC aberrations for which a balancing term, to be added to the primary term, is found, which are defocus, *x*- and *y*-coma, and spherical aberration, as indicated in the third column. In the fourth column, each of the balancing terms has a conjugate term but added to lower-order aberrations. It is obvious that the terms conjugate to the defocus balancing term and one of the two balancing spherical aberration, are added to piston. The terms balancing ZC *x*- and ZC *y*-coma has matching terms added to ZC *x*- and ZC *y*-tilt, respectively. The other balancing term for ZC spherical aberration is matched by a term added to ZC defocus. The last column contains cross terms that indicate the coupling effect between pairs of specific coefficients. This means that the effect of one coefficient of the pair on the variance depends on the value of the other, a process by which higher-order ZC aberrations have an effect on lower-order aberrations. As we will see later, this plays a critical role in the analysis of Zernike-based adaptive methods. Now the sum of the squares of the ZGC coefficients, except piston, gives us the wavefront variance by adding the rest of the terms located from the

second to the fifth columns in the table resulting in Eq. (29). In the process, the balancing terms are cancelled by their conjugate terms except for those matching terms that are added to ZGC piston which, itself, plays no part in the wavefront variance. In a way, we might say that the act of converting ZC to ZGC coefficients can be perceived as a way of decoupling the coupled ZC coefficients. Furthermore, the variance can also be expressed in terms of the classical peak-valley coefficients by replacing each ZC coefficients in Eq. (29) with the equivalent classical coefficients with the rest such as ZC *y*-tilt, ZC *x*-coma, ZC *x*- and ZC *y*-triangular astigmatism coefficients set at zero.

d. Strehl ratio and tolerance of Zernike circle aberrations

To investigate tolerance of the ZC aberrations in a circular Gaussian pupil, we set each ZC coefficient at 0.47 rad. This value is the standard deviation of each ZC aberration corresponding to the aberration tolerance of a nearly diffraction-limited system and corresponds to a Strehl ratio of 0.8 based on the definition of the Strehl ratio given by Eq. (11). It has been established that, for a truncated plane wave, aberration tolerance is independent of aberration type [4]. We examine what happens when the overfill factor is reduced while keeping each of the ZC coefficients, in turn, fixed at 0.47 rad and the rest set at 0 rad. The result is illustrated in Fig. 1(a), which therefore represents the aberration tolerance of the respective ZC aberration. As expected, for a truncated plane wave, the Strehl ratio consistently tends to 0.8 for each aberration. However, the general increase of the Strehl ratio with decreasing overfill factor implies an increase in aberration tolerance, which is now dependent on aberration type. This behaviour is a result of the fact that as $\eta \to 0$, the beam is dominated by light concentrated at the centre of the pupil with very low light level everywhere else. Generally, astigmatic aberrations, whose ZC coefficients are $C_1^{\pm 1}$, $C_2^{\pm 2}$ and $C_3^{\pm 3}$, exhibit the highest tolerance with tolerance monotonically increasing with increasing order number. On the other hand, C_4^0 and $C_3^{\pm 1}$ demonstrate the least tolerance with tolerance decreasing with increasing order number until a minimum is reached when η takes on the values 0.53 and 0.51, respectively, after which it starts to increase. All the aberrations exhibit a monotonic increase in tolerance except for C_4^0 and $C_3^{\pm 1}$ in which the tolerance decreases. We proceed to investigate the tolerance of the ZGC aberrations. This variance can be calculated by taking the square of each ZGC aberration in which each constituent ZC coefficient is, again, set at 0.47 rad. The variance of each of these aberrations is shown in Fig. 1 (b) as a function of the overfill factor. For an overfilled pupil, $S(\eta)$ approaches 0.8 for all aberrations $X_n^m = C_n^m$ in the limit of a uniform pupil. However, at lower η, the dependence on aberration type is very clear. There is a monotonic increase in tolerance, which is apparent in all aberrations except for X_1^1, X_1^{-1} and X_2^0 where there is a local minimum at $\eta = 0.513$. The reason for this behaviour is that this is a result of two ZC aberrations. For example, $X_1^{\pm 1}$ is a function of $C_1^{\pm 1}$ and $C_3^{\pm 1}$, and X_2^0 defocus is a function of C_2^0 defocus and C_4^0.

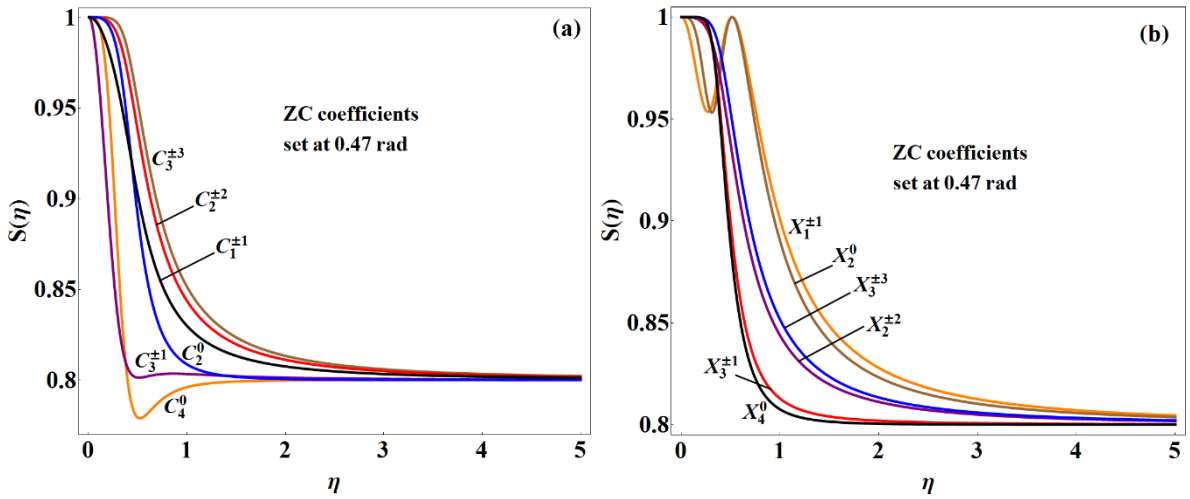

Fig. 1. The amplitude-weighted Strehl ratio as a function of the overfill factor with (a) each ZC coefficients set as 0.47 rad and (b) each ZGC coefficient constructed from ZC coefficients also set at 0.47 rad.

The dependence of η on the primary classical aberrations is tested by setting the respective coefficients, A_4^0, A_3^1, A_2^2, A_2^0 and A_1^1 at 1.58, 1.34, 1.89, 1.64 and 0.95 rad, respectively. Each coefficient values was selected such that in the limit of the overfill factor, the Strehl ratio is 0.8 for each one. The dependence of the Strehl ratio on the overfill factor for each of these aberrations is illustrated in Fig. 2(a). The graph is based on Eq. (27) where each ZC term is expressed in terms of the given primary classical aberration as shown below

$$\sigma_\phi^2 = \beta_{1,1}^1\left(\frac{A_1^1}{2}+\frac{A_3^1}{3}\right)^2 + \frac{\beta_{2,2}^0-(\beta_{2,0}^0)^2}{12}\left(A_2^0+\frac{A_2^2}{2}+A_4^0\right)^2 + \frac{\beta_{2,2}^2}{24}(A_2^2)^2 + \frac{\beta_{3,3}^1}{72}(A_3^1)^2$$
$$+\frac{\beta_{4,4}^0-(\beta_{4,0}^0)^2}{180}(A_4^0)^2 + \frac{\beta_{3,1}^1}{3\sqrt{2}}A_3^1\left(\frac{A_1^1}{2}+\frac{A_3^1}{3}\right) + \frac{\beta_{4,2}^0-\beta_{4,0}^0\beta_{2,0}^0}{6\sqrt{15}}A_4^0\left(A_2^0+\frac{A_2^2}{2}+A_4^0\right). \quad (34)$$

with coefficient values with the rest kept at 0 as η is varied. As η gets smaller, the dependence on aberration coefficients becomes clearer because coma exhibits the highest tolerance while astigmatism exhibits the lowest. The other three curves are located in between those of coma and defocus and exhibit roughly the same tolerance. However, as η decreases further, the tolerance of all the aberrations rises sharply, with coma and spherical aberration showing the steepest increase, followed by astigmatism and defocus, with tilt showing the slowest. The tolerance increases sharply to 1 becoming the same for all aberrations as η is decreased to zero. In Fig. 2(b), we observe the impact of each of the nonzero ZGC coefficients, X_n^m, on $S(\eta)$ as we vary η. These coefficients were built by inserting the classical coefficients into Eq. (24). Each one was then squared and used to calculate an associated value of $S(\eta)$. Note that the values of the classical coefficients are the same as those of Fig. 2(a). The graph shows that $S(\eta)$ is strongly dependent on the aberration type, though it does not depend on η for an overfilled pupil. We see that X_4^0, $X_3^{\pm1}$ and $X_2^{\pm2}$ calculated exclusively from the respective classical aberrations result in a generally low drop in Strehl ratio, levelling off at the respective values of 0.99, 0.98 and 0.86 for large η. This is followed by X_1^1 and then X_2^0, which level of at 0.43 and 0.23, respectively, both of which depend on two different classical aberrations, namely, tilt and coma for X_1^1, and on defocus and spherical aberration for X_2^0. Note that the lower values are, generally, a result of multiple classical aberrations contributing to the ZGC aberrations. As usual, below $\eta = 1$, $S(\eta)$ rises sharply for all aberrations for a truncated plane wave.

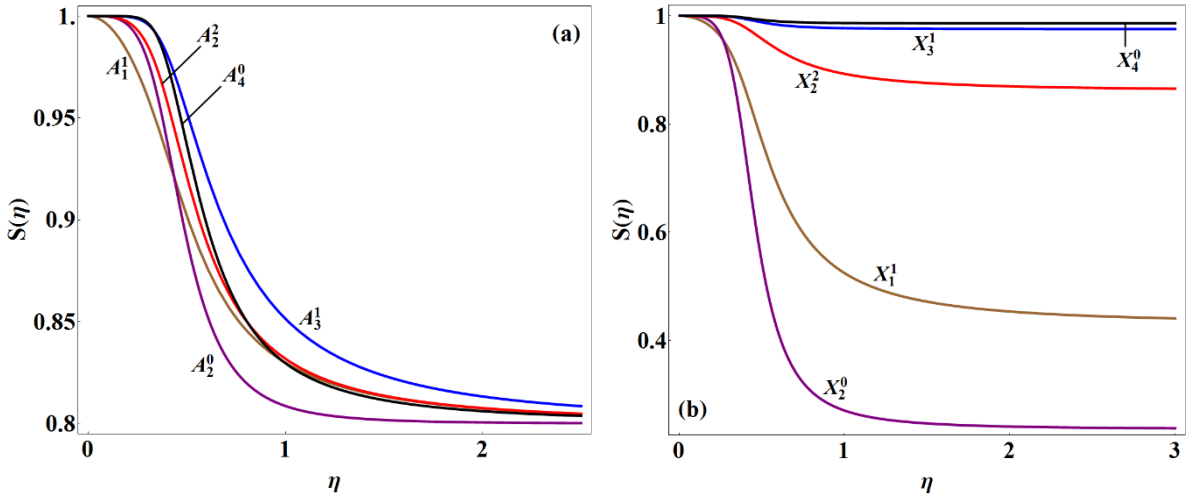

Fig. 2. The amplitude-weighted Strehl ratio as a function of the overfill factor for (a) different primary classical aberrations, each corresponding to a Strehl ratio of 0.8 for a uniform field (b) different ZGC coefficients each one built from the classical coefficients used in Fig. (a).

4. Strehl ratio and Zernike circle aberration correction

We now investigate the validity of using ZGC coefficients for the correction of the Gaussian weighted circular pupil as opposed to using ZC coefficients whilst observing what happens to the Strehl ratio of the PSF as a result. We represent the pupil wavefront variance, σ_ϕ^2, by Eq. (28). After compensating for each aberration in turn, which we depict by setting the respective coefficient, C_n^m to zero, σ_ϕ^2 is expressed as the sum of the square of the remaining coefficients. We start off with the lowest order such that the variance is calculated with the rest, each of which we represent by $C_{n'}^m$ where $n' < n$ up to the highest selected order in the expansion. The validity of using ZGC aberrations for the correction of the Gaussian weighted circular pupil is tested by, first, creating a wavefront in which the first 11 ZC aberration

coefficients were each set at 0.2 rad. The wavefront is then corrected for the ZC and ZGC version of selected aberrations and we compare the respective impact on $S(\eta)$.

The selected aberrations to be investigated here are *x*-tilt and defocus, with the respective results illustrated in Figs. 3(a) and 3(b) by setting them at 0. In each case, a plot of the variation of $S(\eta)$ as a function of η shows that, in general, when a ZGC coefficient is corrected for, $S(\eta)$ increases for all η. However, correcting for the respective ZC coefficient does not always result in an increase in $S(\eta)$ but rather decreases especially when η is above 0.70 and 0.88, as shown in the respective figures. This behaviour is the result of the cross term shown in Table 1. The coupling coefficients of this cross term are shown in Fig 3(c), where, for all η, $\beta_{3,1}^{1} < 0$ and $\beta_{4,2}^{0} - \beta_{4,0}^{0}\beta_{2,0}^{0} < 0$. This means that $S(\eta)$ decreases only when the two coefficients in the cross term are both either positive or negative. An important implication of this result is that if we want to perform the correction using the ZC set, we can correct each pair removing both terms making the cross term, simultaneously, as shown with the dotted curves in Figs. 3(a) and (b). We might refer to these coefficients as coupling coefficients. We see that correcting for tilt and coma as illustrated in Fig. 3(a), and for defocus and spherical aberration in Fig. 3(b), leads in each case to a monotonic increase in $S(\eta)$ for all η. When the pupil becomes overfilled, it makes the balancing due to the pupil non-uniformity unnecessary as the field becomes uniform. However, correcting the other aberrations from ZC *x*-astigmatism to spherical aberration does not decrease $S(\eta)$ because their higher-order counterparts are not part of the fitting process in this case.

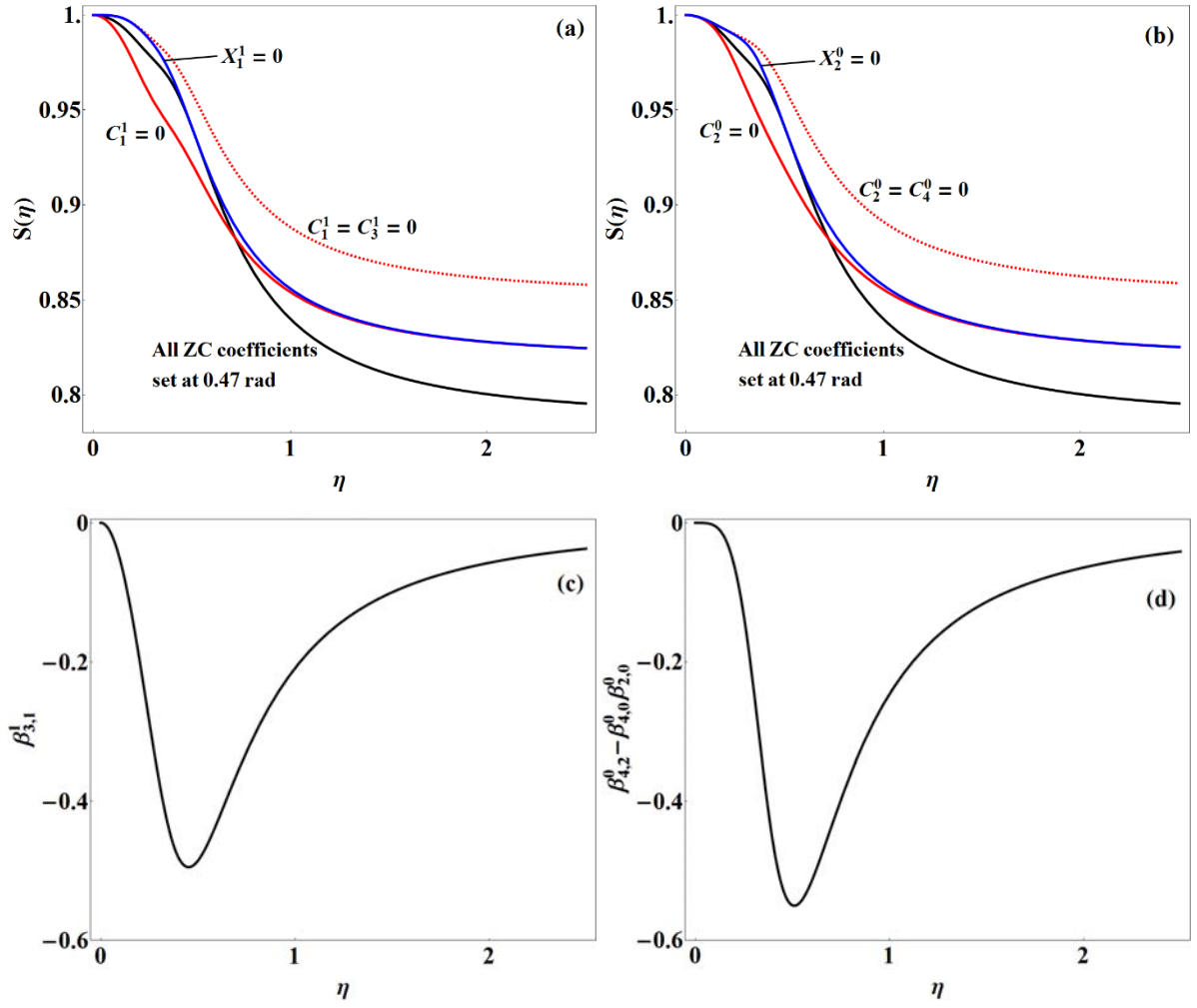

Fig. 3. The amplitude-weighted Strehl ratio as a function of the overfill factor with each ZC coefficient set at 0.2 rad with correction for (a) ZGC and ZC *x*-tilt coefficients, and (b) ZGC and ZC defocus coefficients. (c) The coupling coefficients for the cross terms are shown in Table 1.

We now investigate a system's amplitude-weighted Strehl ratio due to the residual aberration composition after successively correcting for the first j aberrations of the Noll sequence up to $j = J$ using adaptive optics. Let us assume that this Strehl ratio, after correcting up to the Zernike aberration weighted by a coefficient, C_n^m,

corresponding to each j, is given by $\Delta S_{C_n^m}$. We simply set, in turn, the successive ZC coefficients in Eq. (29) to 0, from an initial value of 0.11 rad. The dependence of the result on η is illustrated in Fig. 4(a). Here we observe predictable behaviour when the pupil is overfilled in that as j increases, $S(\eta)$ increases monotonically to reach an ultimate value of 1, where all aberrations have been removed. However, for a strongly underfilled pupil, $S(\eta)$ in general decreases monotonically until it reaches a minimum with *x*-astigmatism, beyond which it starts to increase, again reaching 1. We also make an interesting observation in that all the graphs for ΔS_0 to $\Delta S_{C_2^0}$ intersect at $\eta = 0.7184$ and $S(\eta) = 0.8974$. This indicates that for $\eta = 0.7184$, the Strehl ratio remains constant until *y*-astigmatism has been corrected for and in this case it is unnecessary to correct tilt to defocus.

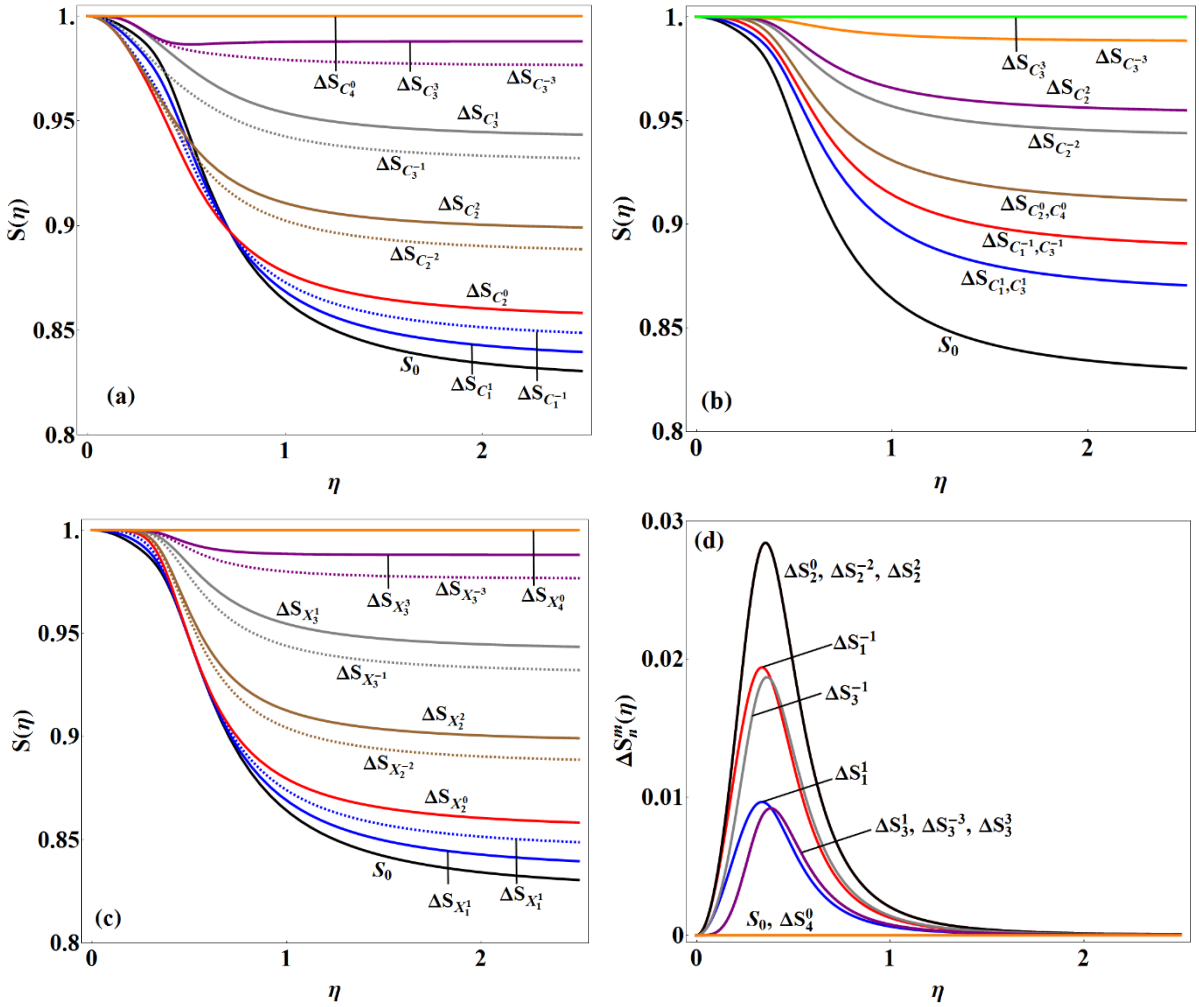

Fig. 4. The residual Strehl ratio from the successive correction of (a) ZC coefficients up to C_n^m, (b) coupled ZC coefficients up to the lower ordered whether coupled or not, (c) ZGC coefficients up to X_n^m. (d) The normalized difference in the residual Strehl ratio, ΔS_n^m, after correcting for each ZCG aberration from correcting the respective ZC coefficient.

Now we consider correcting the non-piston aberrations with the coefficients shown in the mixed terms simultaneously. We opt to pair them up when considering the lower order of each pair. This means that *x*-tilt and *x*-coma are corrected at the same time. Thereafter, *y*-tilt and *y*-coma are corrected and then defocus and spherical aberration. The rest of the aberrations, *y*-astigmatism, *x*-astigmatism, *y*-trefoil, *x*-trefoil, and *x*-astigmatism are corrected for in the pre-set order leading to a Strehl ratio of 1 when all aberrations have been corrected for. The results are illustrated in Fig. 4(b), where it is clear that for all η, $S(\eta)$ increases monotonically as the aberrations are corrected for successively. Fairly similar results can be obtained if the wavefront is, instead, represented in terms of ZGC polynomials. We can proceed to correct for each ZGC aberration in the same order depicted by Noll, the result of which is illustrated in Fig. 4(c). Here, $S(\eta)$ increases monotonically after the correction of each orthonormal

aberration, following the prediction of the orthonormal theory in Section 2. At $\eta \cong 0.5097$, the value of $S(\eta)$ is the same for *x*-tilt, *y*-tilt and defocus. As in Fig. 4(a), this means that at this overfill factor, correction can begin with ZGC *y*-astigmatism instead continuing with the aberrations of increasing order.

The normalized difference after correcting for each successive ZC aberration in the Noll sequence and that of its respective ZGC aberration can be expressed in the form

$$\Delta S_n^m = \frac{\Delta S_{X_n^m} - \Delta S_{C_n^m}}{\Delta S_{C_n^m}}. \tag{35}$$

Eq. (35) illustrates the contrast between using ZGC and ZC polynomials assuming the Noll sequence is followed. For the aberrations selected for this simulation, Fig 4(d) illustrates that using ZGC polynomials results in larger $S(\eta)$ increases for the respective ZC polynomials. For each correction, the largest increase is observed when the pupil is underfilled, which occurs, as already shown, when the ZGC coefficients have maximum utility. As expected when we track ΔS_n^m, we observe that, for $\eta \geq 2$, there is no difference at all between the performance of the two Zernike regimes. However, for an underfilled pupil, $\Delta S_n^m > 0$, with ΔS_n^m increasing from $j = 1$ up to $j = 4$, 5 and 6 before its starts to drop until it becomes 0 when $j = 11$. This confirms that, for an underfilled pupil, the ZGC coefficients achieve higher $S(\eta)$ for each ZGC aberration corrected compared to the same ZC aberration and that the order in which the aberrations are corrected for does not matter.

5. Discussion and conclusion

To characterize a general wavefront, one can either fit the orthonormal Zernike-based polynomials orthonormal in the wavefront to get the respective coefficient set or one can fit the Zernike circle polynomials to get Zernike circle coefficients. With the latter method, we proceed by using Eq. (14) to generate the orthonormal set. With the second option, it is important to note that one does not require the OZ set itself to acquire orthonormal coefficients. In other words, since orthonormal polynomials can be derived using the Gram-Schmidt procedure, we have demonstrated that, instead, the Zernike circle coefficients can be converted to orthonormal coefficients using the Cholesky decomposition, a procedure clearly derived from the Gram-Schmidt procedure and so inherits its nonrecursive properties. At the core of this procedure is a correlation integral in which an inner product of Zernike polynomials is calculated inside the general pupil. The presented model emphasises that if the inner product has an analytical solution, all the coefficients would be analytical too because it serves as the starting point of the Cholesky decomposition, thereby guaranteeing that the rest of the derived coefficients are also analytical.

The model was applied to Zernike circle polynomials inside a Gaussian pupil, which is the main subject of this paper where we have derived an integral of the ZC polynomials in a Gaussian pupil. We used it to establish a relationship between orthonormal coefficients that take into account the Gaussian field and the Zernike circle coefficients that do not. We chose to limit ourselves to the first 11 polynomials according to the Noll sequence. Since Zernike circle coefficients can be related to classical aberrations, this makes it possible to also express orthonormal coefficients in terms of classical aberrations. Since we are limiting ourselves to diffraction-limited systems, the Strehl ratio in the imaging plane can be approximated from the pupil wavefront error, which, in turn, is estimated from the sum of the squares of the non-piston orthonormal coefficients. Consequently, the Strehl ratio, $S(\eta)$, can be expressed in terms of the other coefficients which would allow wavefront analysis with those coefficients too. We used the resulting expressions to confirm that system tolerance is dependent on aberration type for underfilled systems with Zernike circle astigmatic aberrations exhibiting greater tolerance whereas spherical aberration exhibiting the least just below coma. However, the respective orthonormal coefficients determined from the circle coefficients exhibit the same behaviour save for *x*-tilt, *y*-tilt and defocus, which were altered due to the balancing process making the resultant aberrations more tolerant. The sizes of the selected classical aberration were such that the Strehl ratio contribution of each one is 0.8 in the limit of an overfilled pupil. As the overfill factor gets smaller, classical coma achieves greatest tolerance whereas defocus exhibits the least. In the limit of an underfilled pupil, all the aberrations approach the same tolerance except for tilt, which exhibits a value below that of all the others. The respective orthonormal coefficients show that for large η, $S(\eta)$ approaches a constant value that depends on different values of the orthonormal coefficients. However, for small η, the aberrations experience an increase in tolerance in which the aberrations approach 1 at almost the same value of η.

We also looked at the way in which our results can be used to implement aberration correction protocols for a system with a circular Gaussian pupil. We have demonstrated that, in some instances, correcting for aberrations in ZC coefficient form actually reduces the Strehl ratio, whereas correcting for the orthonormal polynomials always results in an increase in the Strehl ratio except in rare occasions, for specific values of η, where it stays the same. We have also confirmed that simultaneously correcting for coupled Zernike circle aberrations results in a monotonic increase in the Strehl ratio without resorting to converting to the orthonormal set. Our investigations into the Strehl

ratio based on the residual wavefront error allowed us to confirm our findings in that we see that if equivalent aberrations are corrected for in ZC form and ZGC form, the latter will result in a larger gain in Strehl ratio.

6. Appendix A: Derivation of the solution to the integral in Eqs. (24)

The first step in solving the integral in the numerator is to separate the radial and angular parts of the ZC polynomials and solving for the denominator to give a somewhat simpler form:

$$\beta_{n,n'}^{|m|} = \frac{2}{\eta^2}\frac{\sqrt{(n+1)(n'+1)}\int_0^1 R_n^{|m|}(\rho)R_{n'}^{|m'|}(\rho)e^{-\rho^2/\eta^2}\rho d\rho}{1-e^{-1/\eta^2}}\delta_{m,m'}. \tag{A1}$$

We proceed to use the following identity on one of the ZC radial polynomial [17]:

$$R_n^{|m|}(\rho) \equiv (-1)^p \int_0^\infty J_{n+1}(r)J_{|m|}(r\rho)dr; \quad 0 \le \rho < 1, \tag{A2}$$

where J_n is the n-th order Bessel function of the first kind, which leads us to

$$\beta_{n,n'}^{|m|} = \delta_{m,m'}\frac{2}{\eta^2}\frac{(-1)^p\sqrt{(n+1)(n'+1)}}{1-e^{-1/\eta^2}}\int_0^\infty J_{n+1}(r)dr\int_0^1 e^{-\rho^2/\eta^2}R_{n'}^{|m|}(\rho)J_{|m|}(r\rho)\rho d\rho. \tag{A3}$$

The solution to the integral over the radial coordinate can be effected using the following formula from the extended Nijboer-Zernike theory [21]:

$$\begin{aligned}&\int_0^1 e^{-\rho^2/\eta^2}R_{n'}^{|m|}(\rho)J_{|m|}(r\rho)\rho d\rho \\ &= e^{-1/\eta^2}\sum_{l=1}^{\infty}\left(\frac{2}{\eta^2}\right)^{l-1}\sum_{s=0}^{p'}(-1)^{p'}(2s+l+|m|)\frac{\binom{s+l+|m|-1}{l-1}\binom{s+l-1}{l-1}\binom{l-1}{p'-s}}{\binom{s+l+q'}{l}}\frac{J_{|m|+l+2s}(r)}{lr^l}.\end{aligned} \tag{A4}$$

Substituting for this result in Eq. (A3) leaves us with one unsolved integral which is given below together with its standard solution [25]:

$$\int_0^\infty \frac{J_{n+1}(r)J_{|m|+l+2s}(r)}{r^l}dr = \frac{(s+q)!}{2^l(s+l+q)!}\binom{l-1}{p-s}. \tag{A5}$$

which is based on the standard integral given by Eq. (6.574-2) on page p. 683 of reference (25). Finally, substituting the result from Eqs. (A4) and (A5) into Eq. (A3), we get the first version of the solution to Eq. (24) after implementing some minor modifications.

An alternative result is acquired when we make the assumption that the upper limit of Eq. (A1) is set at ∞. This condition is repeated in the appropriate subsequent equations. The radial ZC polynomial is replaced by the definition given in Eq. (3) and then the resulting integral to be solved using a standard integral given by Eq. (6.631-1) on page p. 706 of reference (25):

$$\begin{aligned}\int_0^\infty e^{-\rho^2/\eta^2}R_{n'}^{|m|}(\rho,\theta)J_{|m|}(r\rho)\rho d\rho &= \sum_{s=0}^{p'}(-1)^s\binom{n'-s}{s\quad p'-s\quad q'-s}\int_0^\infty e^{-\rho^2/\eta^2}\rho^{n'-2s}J_{|m|}(r\rho)\rho d\rho \\ &= \frac{r^{|m|}}{2^{|m|+1}}\sum_{s=0}^{p'}(-1)^s\binom{n'-s}{s\quad p'-s\quad q'-s}\eta^{2(q'-s+1)}{}_1F_1\left(q'-s+1,|m|+1,-\frac{r^2\eta^2}{4}\right)\end{aligned}, \tag{A6}$$

where ${}_1F_1$ is the confluent hypergeometric function. The result is inserted into Eq. (A3) which itself was derived from Eq. (A2) which is valid inside a unit circle which implies that the final result from is valid within this domain. The last unsolved integral becomes:

$$\int_0^\infty r^{|m|}J_{n+1}(r){}_1\tilde{F}_1\left(q'-s+1,|m|+1,-\frac{r^2\eta^2}{4}\right)dr = \frac{2^{|m|}}{(q'-s)!}G_{2,3}^{2,1}\left(\frac{1}{\eta^2}\middle|\begin{matrix}1 & |m|+1\\ q+1 & q'-s+1 & -p\end{matrix}\right), \tag{A7}$$

which is based in the standard integral given by Eq. (7.542-5) on p. 818 of reference (25) where the confluent hypergeometric function is now regularized. Lastly, after inserting the result from Eqs. (A6) and (A7) into Eq. (A3), the second alternative is realised.

7. Appendix B: Mathematica® code for calculating the mean and wavefront error of a circular Gaussian pupil from Zernike circle coefficients

Various formulae expressed in this paper can be conveniently converted into computer code. All the stages of derivation have been adequately explained to facilitate the conversion. For example, Cholesky decomposition can be implemented using Eq. (19) by implementing the formula as given with a starting condition $g_{11}=1$, then any selected g can be deduced with the calculation continued until the final result is expressed in terms of the β parameters only. This is left as an exercise to the interested reader. In this paper, we limit ourselves to the primary result which is to restore the benefits of normalization. In this paper, we have demonstrated that we do not have to generate ZGC polynomials to fit to the wavefront to get ZGC coefficients. Rather, if we have a wavefront sensor that can give us ZC coefficients, we just need the overfill factor. To that end, the key results in this paper are Eqs. (21), (32) and (34) from which the correct mean and wavefront error are acquired once the coefficients are generated. We have opted to limit ourselves to Eq. (21) as an illustration.

a. Conversion of the β parameter from the double to the single index form

The first step is to express the β parameter in single index form using Eq. (4) which we entered into the second equation of Eq. (24). We altered the β parameter to realise a new expression in which j', n' and m' are replaced by J, v and M, respectively. The code designed to achieve this is given below. The resulting expression, as you might expect, is complicated and takes a lot of space and so cannot be presented here as it requires a lot of space.

```
Clear[j]; Clear[J]; Clear[η];
n = ⌈(√(8 j + 1) - 3)/2⌉;
m = (-1)^(j mod 2) (n - 2 ⌊((n + 1) (n + 2) - 2 j)/4⌋);
v = ⌈(√(8 J + 1) - 3)/2⌉;
M = (-1)^(J mod 2) (v - 2 ⌊((v + 1) (v + 2) - 2 J)/4⌋);
β[j_, J_] := δ_(|m|,|M|) δ_(0,(n-|m|) mod 2,(v-|m|) mod 2) (-1)^((n-|m|)/2) √(n + 1) √(v + 1) / (1 - ε^(-1/η^2))
Sum_(s=0)^((v-|m|)/2) (-1)^s Multinomial[s, (v - |m|)/2 - s, (v + |m|)/2 - s] η^(v+|m|-2 s) G^(2,1)_(2,3)(1/η^2 | (n+|m|)/2 + 1, (v+|m|)/2 - s + 1, -(n-|m|)/2 ; 1, |m| + 1)
β[j, J] // FullSimplify // TraditionalForm
```

b. Mean and wavefront error of a nearly diffraction-limited light from a circular Gaussian pupil calculated from Zernike circle coefficients

The output from the above code now acts as an input for the next part of the calculation where we determine the Strehl ratio of the first 11 coefficients according to Noll sequence. The coefficients are randomly generated and the overfill factor was fixed at, $\eta=0.3$ a value in which the nonuniformity of the field has a clear impact. The resultant mean and wavefront error are 0.0859 λ and 0.0324 λ^2, respectively. These can be compared with 0.002 λ and 0.0621 λ^2, the results which we might get of it was a uniform field instead. The code can be used to verify that the two sets of results would be the same for $\eta=3$ as the Gaussian pupil becomes overfilled and becomes uniform.

```
Clear[η]
β[j_, J_] := %
n = 11;
η = .3;
C1 = 0.002; C2 = 0.001; C3 = −0.003; C4 = 0.0025; C5 = 0.002; C6 = −0.0072; C7 = 0.0092; C8 = −0.00552;
C9 = −0.0212; C10 = 0.0302; C11 = 0.0702;
∑_{j=1}^{n} Cj β(1, j) // FullSimplify // TraditionalForm
∑_{j=2}^{n} ∑_{J=j}^{n} ((β(J, J) − β(1, J)^2) CJ^2 + 2 Cj CJ (1 − δjJ) (β(j, J) − β(1, j) β(1, J))) // FullSimplify // TraditionalForm
C1 // FullSimplify // TraditionalForm
∑_{j=2}^{n} ∑_{J=j}^{n} CJ^2 // FullSimplify // TraditionalForm
```

Out[313]//TraditionalForm=
0.0859114

Out[314]//TraditionalForm=
0.0323804

Out[315]//TraditionalForm=
0.002

Out[316]//TraditionalForm=
0.0621184

References

1. Gu, M.; *Advanced Optical Imaging Theory*, Springer-Verlag Berlin Heidelberg, 2000.
2. Born, M.; Wolf, M.; *Principles of Optics: Electromagnetic Theory of Propagation, Interference and Diffraction of Light*, 7th ed.; Cambridge University Press, Cambridge, 1999.
3. Mahajan, V. N.; *Appl. Opt.* **1995**, *34*, 8057–8059.
4. Mahajan, V. N.; *Optical Imaging and Aberrations, Part II: Wave Diffraction Optics*, 2nd ed.; SPIE, Bellingham Washington 2011.
5. Mafusire, C; Krüger, T. P. J. *Appl. Opt.* **2017** *56*, 2336–2345.
6. Mafusire, C; Kruger, T. P. J. *J. Opt. Soc. Am A*, **2018** *35*, 840.
7. Schwiegerling, J. *J. Opt. Soc. Am A,* **2004** *21,* 2065.
8. Nam, J.; Rubinstein, J. *J. Opt. Soc. Am A,* **2005** *22,* 1709.
9. Liao, K.; Hong. Y.; Sheng. W. *App. Opt.* **2005** *22,* 1824.
10. Mahajan, V. N.; *Optical Imaging and Aberrations, Part III: Wavefront Analysis*, SPIE, Bellingham Washington, 2013.
11. Dai, G.-M.; Mahajan, V. *Opt. Lett.* **2007** *32*, 74–76.
12. Dai, G.-M.; *Wavefront Optics for Vision Correction*, SPIE, Bellingham Washington, 2008.
13. Mahajan, V. N. *Appl. Opt.* **2010** *49*, 5373-5377.
14. Dai, G.-M.; Mahajan, V. *J. Opt. Soc. Am. A*, **2007** *27*, 139-155.
15. Ye, J.; Wang, W; Gao, Z; Liu, Z;, Wang, S; Benítez, P.; Miñano, J. C.; Yuan, Q *Opt. Express* **2015** *23*, 26208–26220.
16. Li, M.; Li, D.; Zhang, C.; Wang, K. E. Q.; Chen, H. *J. Opt. Soc. Am. A* **2015** *32*, 1916–1921.
17. Janssen, A. J. E. M.; *J. Opt. Soc. Am A*, **2002** *19*, 849.
18. Noll, R. J.; *J. Opt. Soc. Am.* **1976** *66* 207–211.
19. Wong, A. K-K.; *Optical imaging in projection microlithography*, SPIE, Bellingham Washington, 2005.
20. Wikipedia, The Free Encyclopaedia, https://en.wikipedia.org/w/index.php?title=Zernike_polynomials&oldid=928614376 (accessed Feb 10, 2020).
21. Mahajan, V. *J. Opt. Soc. Am A,* **2004** *21,* 2065.
22. Watkins, D. S.; *Fundamentals of Matrix Computations*, 2nd ed.; Wiley, New York, 2002.
23. Banachiewicz, T.; *Bull. Intern. Acad. Polon. Sci.* A. **1938** 134–135.
24. Banachiewicz, T.; *Bull. Intern. Acad. Polon. Sci.* A. **1938** 393–401.
25. Gradshteyn, I. S.; Ryzhik, I. M.; *Table of Integrals, Series, and Products*, 7th ed.; Academic Press, 2015.